BES Analysis Memo

ψ' and J/ψ decays to K1 K

Stephen L. Olsen, Daniela Paluselli
University of Hawaii

-ABSTRACT-

We report the results of an analysis of the decays of ψ' and J/ψ to $K_1 K$. We find strong signals for $\psi' \to K_1^+(1270)K^-$ but only an upper limit for $\psi' \to K_1^+(1400)K^-$, in contradiction to expectations from flavor-SU(3) symmetry. In the absence of any PDG entries for $J/\psi \to K_1\overline{K}$ decays, we performed a first measurement using a sample of J/ψ's produced via the cascade decay $\psi' \to \pi^+\pi^- J/\psi$. We find an upper limit for the $J/\psi \to K_1^+(1270)K^-$ decay branching ratio that is well below the 14%-rule extrapolation of our ψ' measurement. In addition, the $J/\psi \to K_1\overline{K}$ decays exhibit a flavor-SU(3) violation that is opposite to that seen for the ψ': the branching fraction for $J/\psi \to K_1(1400)\overline{K}$ decays exceeds that for $J/\psi \to K_1(1270)\overline{K}$. This behavior cannot be accommodated by an adjustment to the singlet-triplet axialvector mixing angle.

1 Expectations

Since the strange members of the two ${}^3P_1$ and ${}^1P_1$ octets, called the K_A and K_B, respectively, do not have definite C-parity, the observed physical states are mixtures of the K_A and K_B quark states. These are identified with the $K_1(1270)$ and the $K_1(1400)$ meson states:

$$K_1(1270) = \cos\theta K_B + \sin\theta K_A \quad (1)$$

$$K_1(1400) = \cos\theta K_A - \sin\theta K_B, \quad (2)$$

where the mixing angle is near $\theta = 45^0$ [4].

The dominant $K_1(1270)$ decay mode are $K\rho$ (Br = 42%) and $K_0^*(1430)\pi$ (Br=28%) and, since the resonance mass $M_{K_1(1270)} = 1.270 \pm 0.090$ GeV is nearly the same as $M_K + M_\rho$ and well below $M_{K_0^*(1430)} + M_\pi$, significant phase space distortions of the line shape are expected.

The $K_1(1400)$ decays almost always to $K^*\pi$ (Br = 92%).

To the extent that flavor-SU(3) is a good symmetry, the amplitude for two body decays to conjugate mesons in the same pair of octets should be equal. Thus, since the $J/\psi(\psi') \to a_1\pi$ decays are forbidden by G-parity, the $J/\psi(\psi') \to K_A\overline{K}$ decays are disallowed and one expects relatively pure $K_B\overline{K}$ final states in J/ψ and ψ' decays. In that case, since

$$K_B = \cos\theta K_1(1270) - \sin\theta K_1(1400), \tag{3}$$

with $\theta \simeq 45^0$, there should be roughly equal amounts of $K_1(1270)$ and $K_1(1400$.)

1.1 Clebsch Gordon coefficients

We search for ψ' and $J/\psi \to K_1^+K^-$ decays where the K_1 decays via $K_1^+ \to K^+\pi^+\pi^-$ in the $K^+K^-\pi^+\pi^-$ event sample. The J/ψ events are extracted from the $\psi' \to \pi\pi J/\psi$ sample.

The $K\rho$ channel is the dominant $K_1(1270)$ decay mode, with a branching fraction of 42 $\pm$ 6% [5]. The isospin decomposition of the $(K\rho)^+$ final state is:

$$(K\rho)^+ = \sqrt{\frac{2}{3}}K^0\rho^+ - \sqrt{\frac{1}{3}}K^+\rho^0 \tag{4}$$

The branching ratio for $\rho^0 \to \pi^+\pi^-$ is essentially 100%.

The $K^*\pi$ channel is the dominant decay mode for the $K_1(1400)$ with a branching fraction of 94$\pm$ 6%. It is also significant for the $K_1(1270)$ where the $Br(K_1(1270) \to K^*\pi) = 16 \pm 5\%$ and the $Br(K_1(1270) \to K_0^*(1430)\pi) = (28 \pm 4)\%$.

The isospin decomposition of the $(K^*\pi)^+$ final state is

$$(K^*\pi)^+ = \sqrt{\frac{2}{3}}K^{*0}\pi^+ - \sqrt{\frac{1}{3}}K^{*+}\pi^0 \tag{5}$$

with

$$K^{*0} = \sqrt{\frac{1}{3}}K^0\pi^0 - \sqrt{\frac{2}{3}}K^+\pi^- \tag{6}$$

$$K^{*+} = \sqrt{\frac{2}{3}}K^0\pi^+ - \sqrt{\frac{1}{3}}K^+\pi^0, \tag{7}$$

In this analysis we consider $J/\psi \to K^+K^-\pi^+\pi^-$ final states. The relevant final states and branching fractions that take the appropriate Clebsch-Gordon coefficients into account are as follows:

$$
\begin{array}{lcccccll}
K_1^+(1270) & \to & K^+\rho^o & \to & K^+\pi^+\pi^- & = & 0.14 \pm 0.02 \\
 & \to & K^{*0}\pi^+ & \to & K^+\pi^+\pi^- & = & 0.07 \pm 0.02 \\
K_1^+(1400) & \to & K^{*0}\pi^+ & \to & K^+\pi^+\pi^- & = & 0.42 \pm 0.03 \\
 & \to & K^+\rho^o & \to & K^+\pi^+\pi^- & = & 0.01 \pm 0.01
\end{array}
$$

1.2 $\psi' \to K^+K^-\pi^+\pi^-$ event selection

1.2.1 Preselection

We select events with four charged tracks in the polar angle region $\mid \cos\theta \mid \leq 0.8$ and with zero net charge. To reduce the number of $\psi' \to \pi^+\pi^- J/\psi$ cascade events where $J/\psi \to \ell^+\ell^-$, we veto events where both the highest momentum positive and negative tracks are identified as muons or where they *both* have a BSC energy deposit that is greater than 0.8 GeV.

The four charged tracks are subjected to a 4-constraint kinematic fit to the $\psi' \to K^+K^-\pi^+\pi^-$ hypothesis for each of the four possible particle assignment combinations and select the assignment with the best χ^2 value. We keep the 12691 events with $\chi^2 \leq 50$ and write them into a Ntuple file for further analysis. Included in the Ntuple file is the χ^2 value returned from a 4-c fit to the hypothesis $\psi' \to \mu^+\mu^-\pi^+\pi^-$, where the highest momentum positive and negative tracks are taken to be the μ^+ and μ^-.

1.2.2 Final selection

The following selection criteria are applied to extract the final sample of $\psi' \to K_1^+K^-$ event candidates:

$\chi^2_{\mu^+\mu^-\pi^+\pi^-} > \chi^2_{K^+K^-\pi^+\pi^-}$: Figure 1a shows the distribution of χ^2 values for the fit of the events to the $\psi' \to \mu^+\mu^-\pi^+\pi^-$ hypothesis. We reject events where this fit is better than the $K^+K^-\pi^+\pi^-$ fit.

$\chi^2_{K^+K^-\pi^+\pi^-} < 12.$: Figure 1b shows the distribution of χ^2values for the $K^+K^-\pi^+\pi^-$ hypothesis. We keep events with $\chi^2 < 12$.

$M_{\pi^+\pi^-} \leq 2.4$ GeV : Figure 1c shows the distribution of the invariant mass of the tracks assigned as the π^+ and π^-. The peak near $M_{\pi^+\pi^-} = 2.4$ GeV corresponds to events of the type $\psi' \to \pi^+\pi^- J/\psi$; with $J/\psi \to p\bar{p}$ where the cascade pions are misassigned as kaons and the $p\bar{p}$ are misassigned as pions. This cut eliminates these events with essentially no loss of $K_1\overline{K}$ signal.

$1.05 \leq M_{K^+K^-} \leq 3.0$ GeV : Figure 1d shows the distribution of the invariant mass of the tracks assigned as the K^+ and K^-. The peak near $M_{K^+K^-} = 3.1$ GeV correspond to events of the type $\psi' \rightarrow \pi^+\pi^- J/\psi$ where the J/ψ decays to two charged tracks. (This peak correlates with the low mass peak in the $M_{\pi^+\pi^-}$ distribution shown in Fig. 1c.) Not as clear in this plot is a small peak at low K^+K^- masses corresponding to $\phi \rightarrow K^+K^-$. This cut eliminates these events with a little loss of $K_1\overline{K}$ signal.

$X_{\pi k}^{K^\pm} > 0.1$: Here

$$X_{\pi k} = \frac{weight_k}{weight_\pi + weight_k}, \tag{8}$$

where $weight_i$ are the values assigned by the particle identification system (pid) to the hypothesis $i = \pi$ or K. This eliminates events where the pid unambiguously identifies as a pion a particle that the 4-c fit assigned as a kaon.

We use the IHEP Particle ID package for the psiprime data, and the Mike Kelsey's Particle ID package for the 4.03 GeV data.

$\mid cos\theta \mid > 0.75$: where θ is the helicity angle. In the $K_1(1270)$ rest frame, θ is defined as the angle between the ρ^0 and the K^- recoiling from the $K_1^+(1270)$.

In the $K_1^+(1400)$ rest frame, it is defined as the angle between the K^{*0} and the K^- recoiling from the $K_1^+(1400)$.

This cut eliminates the background reflection at higher masses, due to the wrong combinations of $K^\pm\pi^+\pi^-$ See Monte Carlo Figures 2.

$\mid CL_{TOF}^{\pi\pi kk} \mid$ **or** $\mid CL_{Dedx}^{\pi\pi kk} \mid > 0.05$: for the ψ' data. (Li Xin Hua and Bill Dunwoodie Particle ID package) This package has been used on the psiprime data only, because it is not available for the Monte Carlo. Its results are compatible with the ones obtained with the IHEP package.

A total of 488 events satisfy our selection requirements.

1.3 $\psi' \rightarrow K^+K^-\pi^+\pi^-$ invariant mass distributions

Figure 3a shows a scatterplot of $\pi^+\pi^-$ (vertical) $K^\pm\pi^+\pi^-$ (horizontal) masses for the selected events (two entries per event). The $\rho(770)$ shows up as a horizontal band in the scatterplot; a clustering of events at the left edge of this band indicates the presence of a $K_1(1270)$ signal. Figure 3b shows the $\pi^+\pi^-$ mass distribution. The $\rho(770)$ shows up as an obvious peak. Figure 3c shows the $K^\pm\rho^0$ mass distribution, where the ρ^0 is

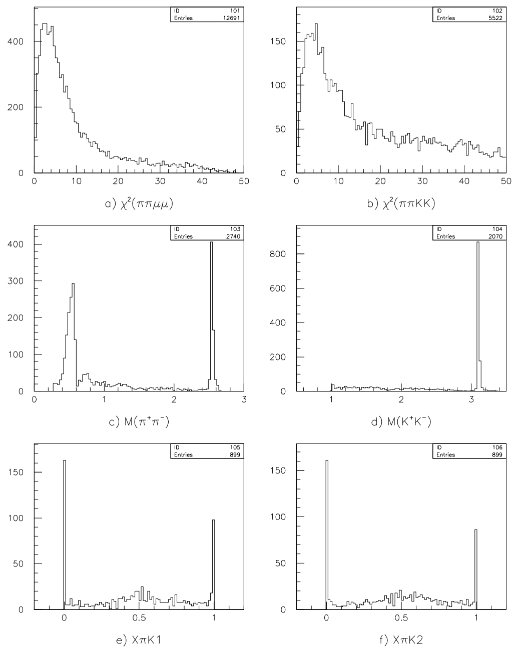

Figure 1: Distributions of precut values of the variables used for the $\psi' \to K^+K^-\pi^+\pi^-$ selection.

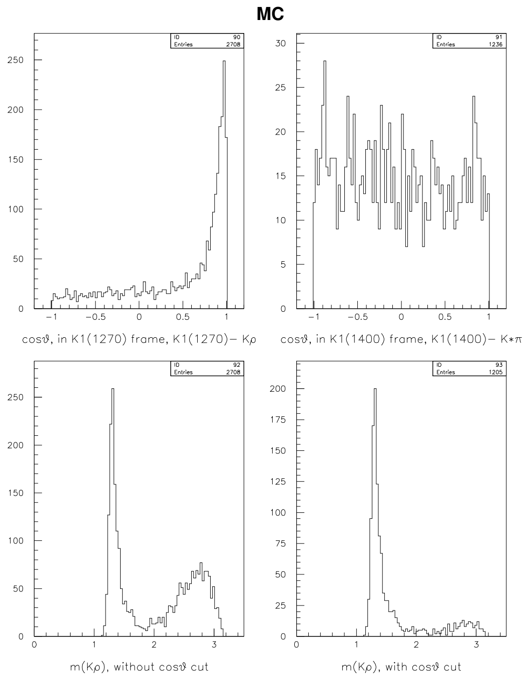

Figure 2: MC: Helicity angle distributions.

taken to be $\pi^+\pi^-$ pairs within ± 0.150 GeV of the nominal ρ mass. A peak at low $M_{K\rho}$ values is prominent.

Figure 3d shows a scatterplot of $K^\pm\pi^\mp$ (vertical) vs $K^\pm\pi^+\pi^-$ (horizontal) masses for the selected events (four entries/event). The $K^*(890)$ shows up as a horizontal band. Figure 3e shows the $K^\pm\pi^\mp$ mass distribution (two entries/event) where the $K^*(890)$ shows up as an obvious peak. Figure 3f shows the $K^{*0}\pi^\pm$ mass distribution, where the K^* is taken to be $K^\pm\pi^\mp$ pairs within ± 0.050 GeV of the nominal K^{*0} mass. There is some peaking of events near low M_K values. There is not much evidence for the $K_1(1400)$, even though the $K^*\pi$ channel is its dominant decay mode. The same analysis performed on the 4.03 GeV data is shown in Fig. 4.

2 Fits to the $K^\pm\rho$ mass distributions.

2.1 Signal and Background

As noted above, the restricted phase space for the $K_1(1270) \to K\rho$ decay is expected to distort the resonance shape for this mode. We, therefore, fit the $K^\pm\rho$ mass distribution of Fig. 3c to specially devised function $f_{K\rho}$ that explicitly takes these distortions into account [9]. This function is the convolution an s-wave Breit Wigner function with mass and width fixed at the PDG values for the $K_1(1270)$ ($M_{K1} = 1.270$ GeV and $\Gamma_{K1} = 0.090$ GeV) with a p-wave ρ meson Breit Wigner with $M_\rho = 0.77$ GeV and $\Gamma_\rho = 0.150$ GeV. Specifically,

$$f_{K\rho}(M_{K\pi\pi}) = \frac{A q^*_{K\pi\pi}}{(M^2_{K1} - M^2_{K\pi\pi})^2 + M^2_{K1}\Gamma^2_{K1}} \int_{M^{min}_{\pi\pi}}^{M^{max}_{\pi\pi}} \frac{q^*_K (q^*_\pi/q^0_\pi)^3 \Theta(M_{K\pi\pi} - M_K - M_{\pi\pi}) dM_{\pi\pi}}{(M^2_\rho - M^2_{\pi\pi})^2 + M^2_\rho[\Gamma_\rho(q^*_\pi/q^0_\pi)^3]^2} \tag{9}$$

where:

$q^*_{K\pi\pi}$ is the momentum of the $K\pi\pi$ system in the ψ' rest frame;

$M^{min}_{\pi\pi}$ and $M^{max}_{\pi\pi}$ are the lower and upper limits of the ρ mass selection;

q^*_K is the momentum of the K in the $K\pi\pi$ rest frame;

q^*_π is the π momentum in the $\pi\pi$ rest frame;

q^0_π is the π momentum in the $\pi\pi$ rest frame for $M_{\pi\pi} = M_\rho$;

$\Theta(x > 0) = 1$ and $\Theta(x < 0) = 0$.

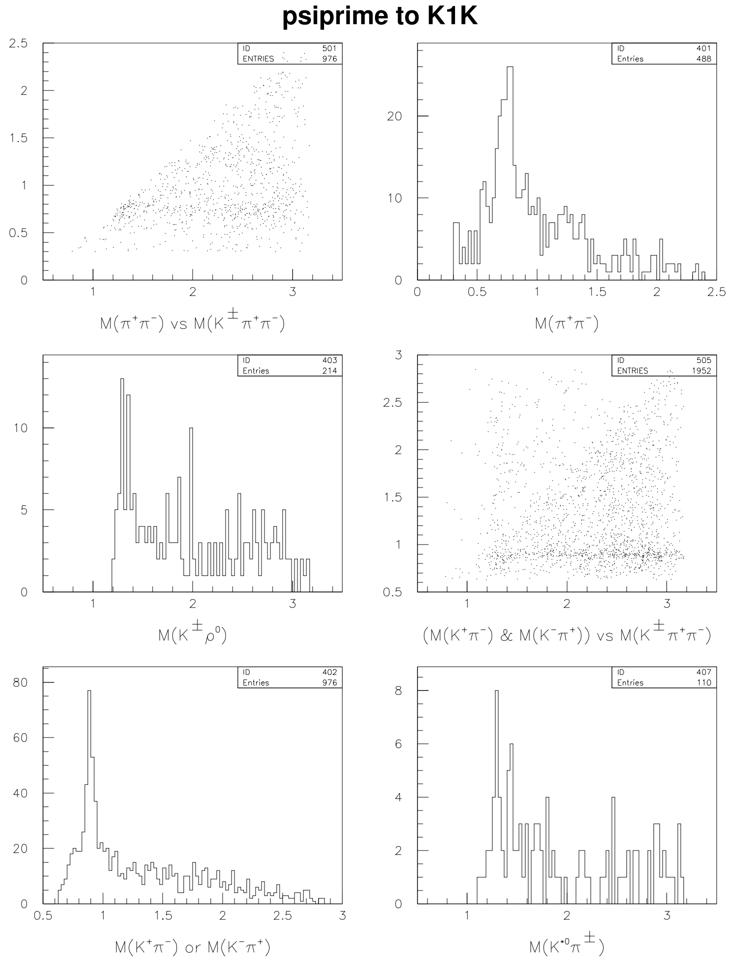

Figure 3: Psiprime data, $L_{in} = 6.1pb^{-1}$: **a)** A scatterplot of $\pi^+\pi^-$ (vertical) vs $K^\pm\pi^+\pi^-$ (horizontal) masses for selected events. The **b)** $\pi^+\pi^-$ and **c)** $K\rho$ mass distributions. **d)** A scatterplot of $K^\pm\pi^\mp$ (vertical) vs $K^\pm\pi^+\pi^-$ (horizontal) masses for selected events. The **e)** $K\pi$ and **f)** $K^*\pi$ mass distributions.

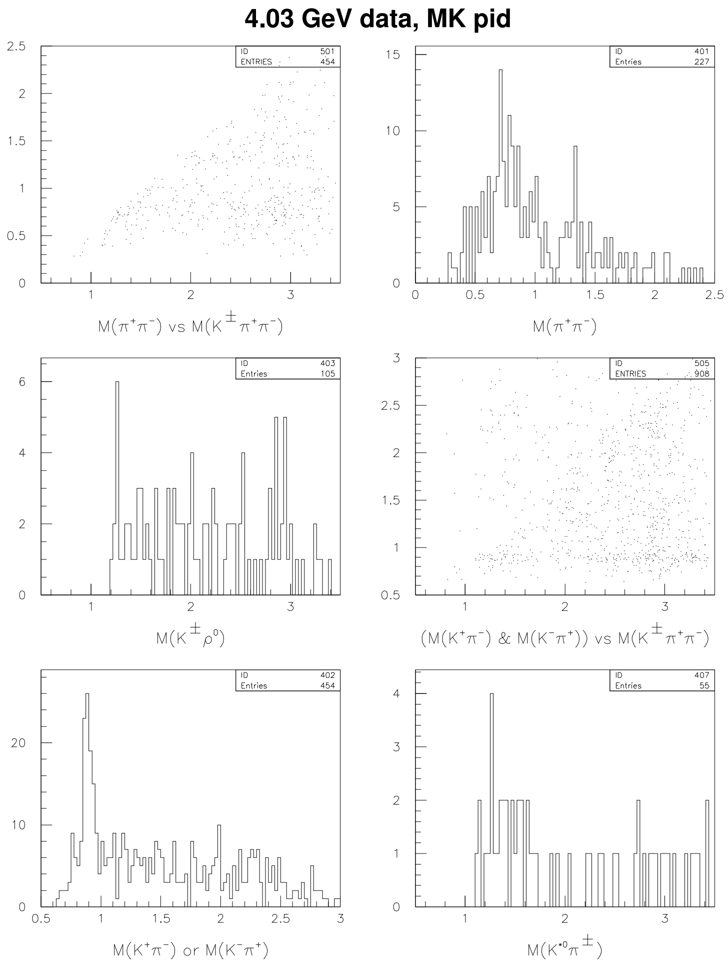

Figure 4: 4.03 GeV data, $L_{in} = 22.3pb^{-1}$: **a)** A scatterplot of $\pi^+\pi^-$ (vertical) vs $K^\pm\pi^+\pi^-$ (horizontal) masses for selected events. The **b)** $\pi^+\pi^-$ and **c)** $K\rho$ mass distributions. **d)** A scatterplot of $K^\pm\pi^\mp$ (vertical) vs $K^\pm\pi^+\pi^-$ (horizontal) masses for selected events. The **e)** $K\pi$ and **f)** $K^*\pi$ mass distributions.

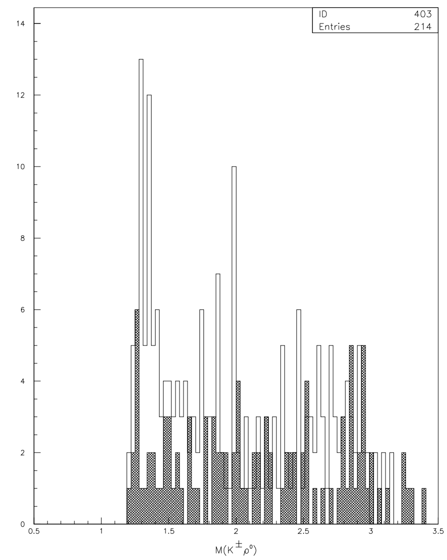

Figure 5: 4.03 GeV continuum ($L_{int} = 22.3pb^{-1}$), superimposed on ψ' data distribution ($L_{int} = 6.1pb^{-1}$).

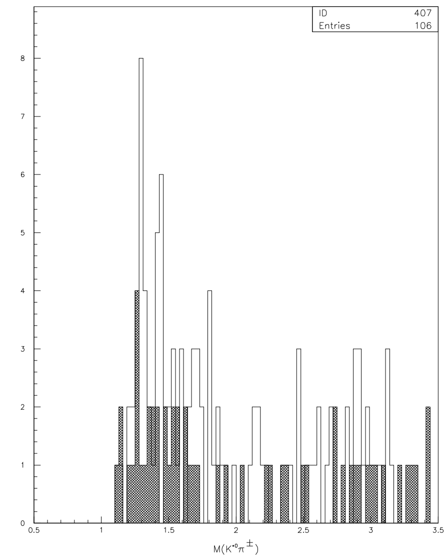

Figure 6: 4.03 GeV continuum ($L_{int} = 22.3pb^{-1}$), superimposed on ψ' data distribution ($L_{int} = 6.1pb^{-1}$).

Given the mass cuts listed above, the only free parameter for this function is the overall normalization.

We add to the resonance Breit Wigner a smooth curve of the form

$$\begin{aligned} f_{bkg}(Q) &= p_1(Q^{\frac{1}{2}} + p_2 Q^{3/2} + p_3 Q^{5/2}) \quad Q > 0 \\ &= 0 \qquad\qquad\qquad\qquad\qquad\quad Q \leq 0, \end{aligned} \tag{10}$$

where $Q \equiv M - (M_K + M_\rho)$. The fit region is restricted to $0.5 \leq M(K\rho) \leq 3.0$ GeV for the ψ' data and to $0.5 \leq M(K\rho) \leq 2.5$ GeV for J/ψ. The number of events will be calculated as the integral of the signal between 1.0 and 2.0 GeV, both for the data and the Montecarlo. These limits are used also in the fit to the $K^*\pi$ distribution.

2.2 Fit results

The above functions are used to fit the entire mass distribution for $\psi' \to K_1(1270)K$. The result of the fit between 0.5 and 2.5 GeV, in a plot extended from 0.5 to 3.0 GeV, gives $N_{evt}^{K_1(1270)} = 54.3 \pm 14.1$ when using the IHEP particle identification package, and $N_{evt}^{K_1(1270)} = 54.2 \pm 14.0$ if we use the SLAC package. The results are compatible with each other. We choose the IHEP method, because at the moment the SLAC method is not available for the Monte Carlo. After applying the helicity angle cut, we obtain $N_{evt}^{K_1(1270)} = 44.8 \pm 10.4$. See Fig. 7.

3 $\psi' \to K_1^+ K^-$ acceptance

The detector acceptance and the efficiency for the analysis cuts are evaluated by means of a sample of simulated Monte Carlo events. We generated $20,000$ $\psi' \to K_1^+(1270)K^-$ decays with flat angular distributions. 10,000 events had $K_1^+(1270)$ decaying to $K^+\rho^0$, $\rho^0 \to \pi^+\pi^-$ and 10,000 to $K^{*0}\pi$, $K^{*0} \to K^+\pi^-$. In addition, we generated 10,000 $\psi' \to K_1^+(1400)K^-$ with subsequent $K_1^+(1400) \to K^{*0}\pi$, $K^{*0} \to K^+\pi^-$ decays, also with flat angular distributions. The generated events were passed through a Monte Carlo simulation of the BES detector that generates simulated detector responses. The simulated data are analyzed by the same programs that are used for the data. The $K\rho$ mass distribution for the events in the first sample that survive all the cuts is fit to the $f_{K\rho}$ function, yielding an acceptance for this mode of $\eta_{K\rho}^{K_1(1270)\to K\rho} = 0.089 \pm 0.004$. (see Fig. 9)

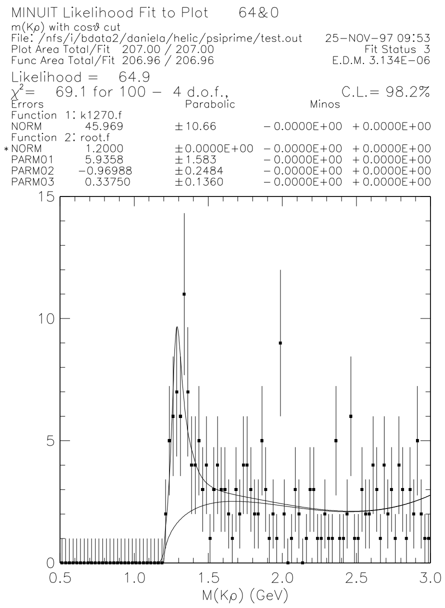

Figure 7: ψ' Data: Fit to the $K^{\pm}\rho^0$ mass distribution using the function $f_{K\rho}$ for the $K_1(1270)$ line shape and f_{bkg} to parameterize the background. IHEP (YUANCZ) pid.

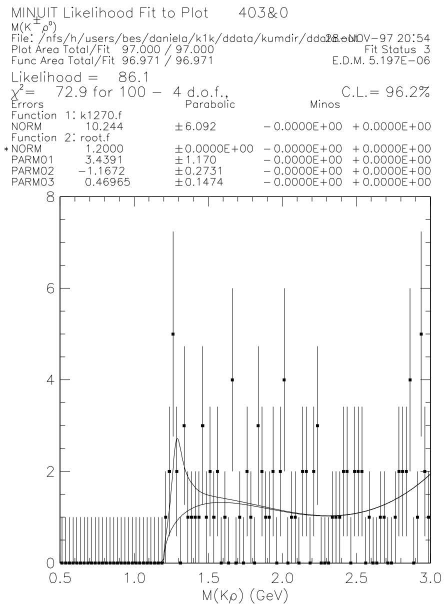

Figure 8: 4.03 GeV Data: Fit to the $K^{\pm}\rho^0$ mass distribution using the function $f_{K\rho}$ for the $K_1(1270)$ line shape and f_{bkg} to parameterize the background. (MK pid).

$K_1(1270)$ can also decay to $K^*\pi$, and the $K\rho$ and $K^*\pi$ cuts are not mutually exclusive. Therefore some of the $K_1(1270)$ in the $K\rho$ distribution, is due to the $K^*\pi$. The efficiency of this contribution is $\eta^{K_1(1270)\to K^*\pi}_{K*\pi/K\rho} = 0.043 \pm 0.002$. (see Fig. 11)

Consistently with the above notation, we find: $\eta^{K_1(1270)\to K^*\pi}_{K^*\pi} = 0.095 \pm 0.003$ (see Fig. 12, where the Breit Wigner is integrated between the limits of 1.0 and 2.0 GeV) and $\eta^{K_1(1270)\to K\rho}_{K\rho/K^*\pi} = 0.029 \pm 0.002$ (see Fig. 10).

The $K^*\pi$ mass distribution from the $K_1(1400)$ sample are fit to an s-wave Breit Wigner function, with parameters fixed at the PDG values. The acceptance is $\eta^{K_1(1400)\to K^*\pi}_{K^*\pi} = 0.084 \pm 0.003$ (see Fig. 13).

To recapitulate:
$\eta^{K_1(1270)\to K\rho}_{K\rho} = 0.089 \pm 0.004$ (10,000 events)
$\eta^{K_1(1270)\to K\rho}_{K\rho/K^*\pi} = 0.029 \pm 0.002$ (10,000 events)
$\eta^{K_1(1270)\to K^*\pi}_{K^*\pi/K\rho} = 0.043 \pm 0.002$ (10,000 events)
$\eta^{K_1(1270)\to K^*\pi}_{K^*\pi} = 0.095 \pm 0.003$ (10,000 events)
$\eta^{K_1(1400)\to K^*\pi}_{K^*\pi} = 0.084 \pm 0.003$ (10,000 events)

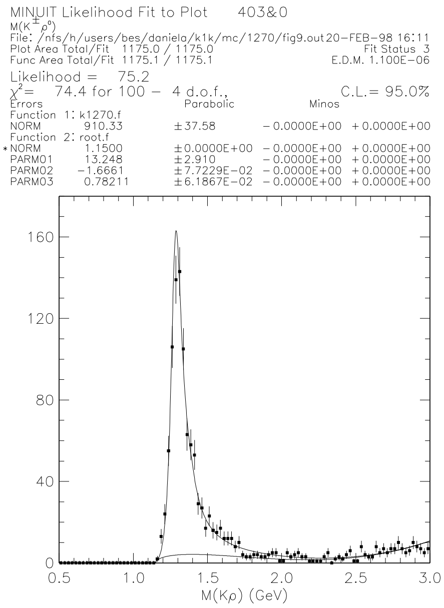

Figure 9: MC $\psi' \to K_1(1270)K$, $K_1(1270) \to K\rho^0$, fit to the $K\rho^0$. (10,000 events)

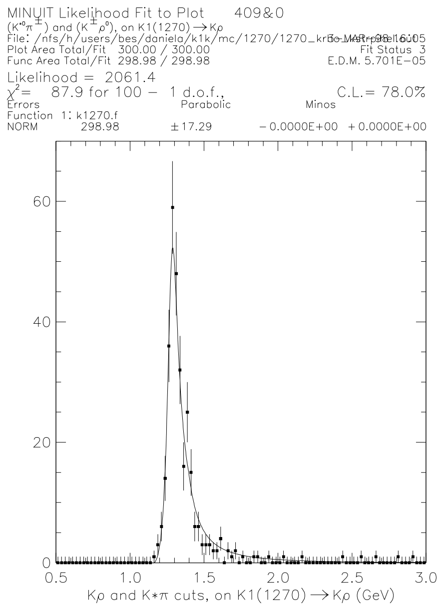

Figure 10: MC $\psi' \to K_1(1270)K$, $K_1(1270) \to K\rho^0$, fit to the $K^*\pi$. (10,000 events)

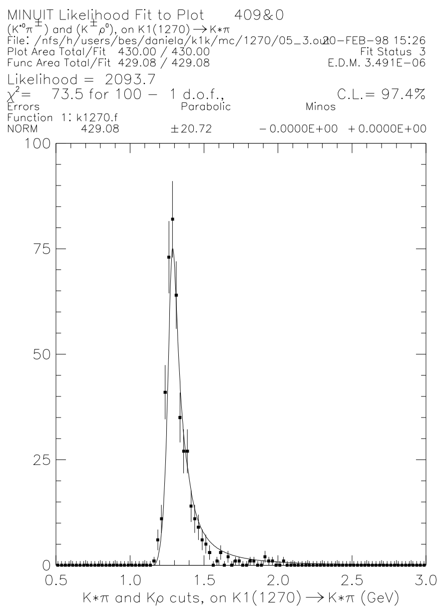

Figure 11: MC $\psi' \to K_1(1270)K$, $K_1(1270) \to K^{*0}\pi^{\pm}$, fit to the $K\rho^0$. (10,000 events)

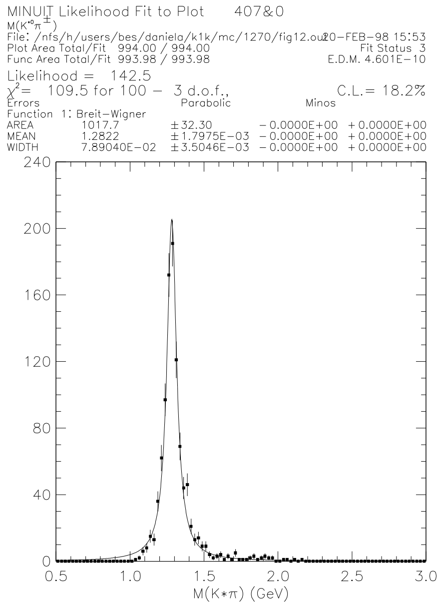

Figure 12: MC $\psi' \to K_1(1270)K$, $K_1(1270) \to K^{*0}\pi^{\pm}$, fit to the $K^{*0}\pi^{\pm}$. (10,000 events)

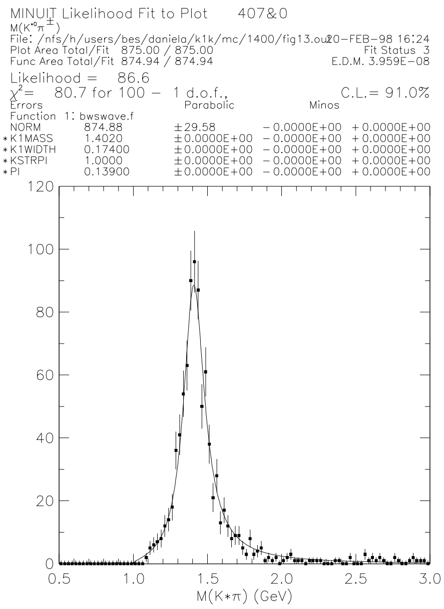

Figure 13: MC $\psi' \to K_1(1400)K$, fit to the $K^{*0}\pi^{\pm}$ mass distribution. (10,000 events)

Table 1: A tabulation of the K_1K selection cuts (not updated with the helicity cut).

Numbers of events surviving each requirement

	94 +95 Data	Simulated events	
		$K_1(1270) \to K^+\rho^0$	$K_1(1400) \to K^{*0}\pi^+$
Preselection:			
Generated		10,000	10,000
4 chrgd trks		6498	6494
$\sum q = 0$		6168	6193
pass $\mu^+\mu^-$ veto	887580	6141	6169
pass e^+e^- veto	846159	6116	6131
$\lvert\cos\theta_{chg}\rvert \leq 0.8$	591100	4484	4292
$\chi^2_{4c} \leq 50$	12691	3326	3227
Selection:			
$\chi^2_{\mu\mu\pi\pi} > \chi^2_{KK\pi\pi}$	5522	3250	3143
$\chi^2_{KK\pi\pi} \leq 12$	2740	2849	2768
$M_{\pi^+\pi^-} < 2.4$ GeV	2170	2845	2765
$1.05 < M_{K^+K^-} < 3.0$ GeV	899	2737	2595
$\lvert X_{\pi K}^{K^+K^-}\rvert > 0.1$	487	1933	1771
Mass cuts:			
$\lvert M_{\pi^+\pi^-} - M_\rho\rvert \leq 0.15$GeV	400	1354	
$\lvert M_{K\pi} - M_{K^*}\rvert \leq 0.05$GeV	205	634	1234

4 $\psi' \to K_1(1270)^+K^-$ (via $K\rho$), branching ratio

Using the relation

$$Br(\psi' \;\to\; K_1^+(1270)K^- \;+\; cc); \qquad via \;\; (K_1(1270) \to K\rho) \tag{11}$$

$$= \frac{N_{evts}^{(1270)}}{N_{\psi'}[\eta_{K\rho}^{(K_1(1270)\to K\rho)} Br_{K_1(1270)\to K\rho \to K^+\pi^+\pi^-} + \eta_{K*\pi/K\rho}^{(K_1(1270)\to K^*\pi)} Br_{K_1(1270)\to K^*\pi \to K^+\pi^+\pi^-}]} \tag{12}$$

we determine the branching ratio result

$$Br(\psi' \to K_1^+(1270)K^- \;+\; cc) = (8.4 \pm 1.9 \pm 1.7) \times 10^{-4}. \tag{13}$$

The statistical error is based on the error on $N_{evts}^{(1270)}$, as obtained from the fit. As shown in Fig. 8, the fit to the continuum distribution for the 4.03 GeV data, yields a value of $N_{evts}^{(1270)} = 10.0 \pm 6.0$. Scaling this number with the luminosities $L_{4.03GeV} = 22.3pb^{-1}$ and $L_{3.686GeV} = 6.1pb^{-1}$ (related errors are less than one percent), and with the square of the relative center of mass energies, we conclude that 3.3 ± 2.0 events of the signal are due to the continuum distribution. The r.m.s. of this contribution (7.3%), with the errors related to the terms in the denominator of the branching fraction, (17%), is taken as the estimate of the systematic error.

5 $\psi' \to K_1(1400)^+K^-$, and $\psi' \to K_1(1270)^+K^-$ (via $K^*\pi$)

We fit the region $K^{*0}\pi^\pm$ mass distribution (Fig. 14) below 3.0 GeV to $f_K\rho$, plus an s-wave Breit Wigner with mass and width fixed at the PDG values for the K_1 (1400) ($m_{K1} = 1.402$ GeV and $\Gamma_{K1} = 0.174$ GeV). We add the same background function used for the $K\rho$ distribution. The resulting fit gives 21.6 ± 9.2 $K_1(1400)$ events, and 17.2 ± 7.3 $K_1(1270)$ events. Since the mass distribution can be fit without either a $K_1(1400)$ ($CL = 89.1\%$), or a $K_1(1270)$ ($CL = 29\%$), we use these number to derive a 90% CL upper limit of $N_{limit}^{(1400)} < 33.4$ (90% CL), and $N_{limit}^{(1270)} < 26.5$ (90% CL).

5.1 $\psi' \to K_1(1270)^+K^-$ (via $K^*\pi$), branching ratio

Using the relation

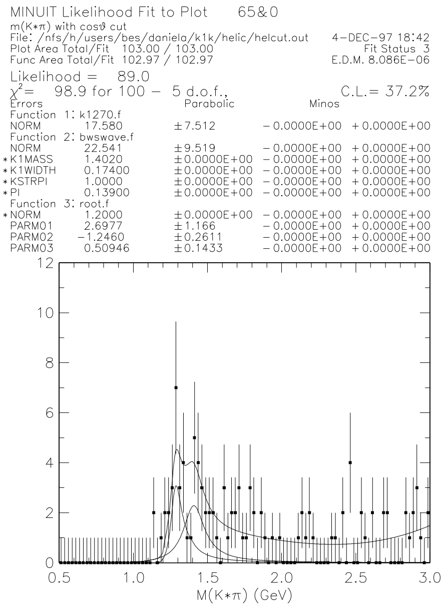

Figure 14: ψ' Data: Fit to the $K^{*0}\pi^{\pm}$ mass distribution.

$$Br(\psi' \;\rightarrow\; K_1^+(1270)K^- \;+\; cc); \qquad via \;\; (K_1(1270) \rightarrow K^*\pi) \tag{14}$$

$$= \frac{N_{evts}^{(1270)}}{N_{\psi'}[\eta_{K\rho K^*\pi}^{(K_1(1270)\rightarrow K\rho)} Br_{K_1(1270)\rightarrow K\rho\rightarrow K^+\pi^+\pi^-} + \eta_{K^*\pi}^{(K_1(1270)\rightarrow K^*\pi)} Br_{K_1(1270)\rightarrow K^*\pi\rightarrow K^+\pi^+\pi^-}]} \tag{15}$$

we find:

$$Br(\psi' \rightarrow K_1^+(1270)K^- \;+\; cc) < 7.3 \times 10^{-4}. \tag{16}$$

which is consistent, within error, with the $Br(\psi' \rightarrow K_1^+(1270)K^- \;+\; cc)$ calculated via $K\rho$.

5.2 $\psi' \rightarrow K_1(1400)^+K^-$ branching ratio

We establish a 90% CL upper limit for the $\psi' \rightarrow K_1(1400)^+K^-$ (+ cc) branching ratio from the relation

$$Br(\psi' \rightarrow K_1^+(1400)K^- \;+\; cc) < \frac{N_{limit}^{(1400)}}{N_{\psi'}\eta_{K^*\pi}^{(1400)} Br_{K_1(1400)\rightarrow K^*\pi\rightarrow K^+\pi^+\pi^-}}, \tag{17}$$

with the result

$$Br(\psi' \to K_1^+(1400)K^- \ + \ cc) < 2.7 \times 10^{-4} \quad 90\% \text{ CL.} \tag{18}$$

Contrary to the flavor-SU(3) expectation of equal amounts of $K_1(1270)$ and $K_1(1400)$, the $K_1(1400)$ mode is smaller than the $K_1(1270)K$ mode by at least a factor of three. There are no PDG entries for these modes for the J/ψ for comparison.

6 $J/\psi \to K_1(1270)K$ and $K_1(1400)K$

For the $\psi' \to K_1^+(1270)K^-$, we see a branching ratio of $(8.4 \pm 1.9 \pm 1.7) \times 10^{-4}$, which is quite large for an exclusive hadronic ψ' decay channel. We do not see a comparable signal for $\psi' \to K_1^+(1400)K^-$, although this is what is expected from flavor-SU(3). According to the 14% rule, the corresponding branching fraction for the J/ψ, should be around 0.64%, which would make it one of the most prominent exclusive hadronic decay channels. The absence of any PDG entries for $J/\psi \to K_1(1270)K$ or $K_1(1400)K$ makes one suspicious that this may not be the case. We used the $\psi' \to \pi^+\pi^- J/\psi$ cascade events in our ψ' data sample to make a first measurement of branching ratios for $J/\psi \to K_1(1270)\overline{K}$ and $K_1(1400)\overline{K}$.

6.1 $\psi' \to \pi^+\pi^- J/\psi; J/\psi \to K^+K^-\pi^+\pi^-$ event selection

6.1.1 Preselection

We select events with six charged tracks in the polar angle region $|\cos\theta| \leq 0.8$ and with zero net charge. No criteria is used on the number or quality of neutral tracks. The six tracks are subjected to a 5-constraint kinematic fit to the $\psi' \to \pi^+\pi^- J/\psi; J/\psi \to K + K^-\pi^+\pi^-$ hypothesis where each of nine neutral particle pairs are tried as the K^+ and K^- combination, and the remaining lowest momentum positive and negative tracks are assigned to be the cascade pions. We select the assignment with the best χ^2 value. We keep the 1901 events with $\chi^2 \leq 50$ and write them into a Ntuple file for further analysis.

6.1.2 Final selection

The following selection criteria are applied to extract the final sample of $J/\psi \to K_1^+K^-$ event candidates:

χ^2_{5c} $< 15.$: Figure 15a shows the distribution of χ^2 values for the $\psi' \to \pi^+\pi^- J/\psi; J/\psi \to K^+K^-\pi^+\pi^-$ hypothesis. We keep events with $\chi^2 < 15$.

$X_{\pi k}^{K\pm} > 0.1$: Figures 15b and c show the $X_{\pi k}$ distribution for the tracks assigned as the K^- and K^+, respectively, where $X_{\pi k}$ is the relative K-π weight assigned by the particle identification system. This eliminates events where the pid unambiguously identifies as a pion a particle that the 5-c fit assigned as a kaon.

$\mid cos\theta \mid > 0.75$: where θ is the helicity angle. In the $K_1(1270)$ rest frame, θ is defined as the angle between the ρ^0 and the K^- recoiling from the $K_1^+(1270)$.
In the $K_1^+(1400)$ rest frame, it is defined as the angle between the K^{*0} and the K^- recoiling from the $K_1^+(1400)$.
This cut eliminates the reflection at higher masses, due to the wrong combinations of $K^\pm\pi^+\pi^-$ See Figures 15e and 15f.

A total of 465 events satisfy these selection requirements. As in the ψ' study, the integral between 1.0 and 2.0 GeV will be used as estimate of the signal, both for the Montecarlo and the data.

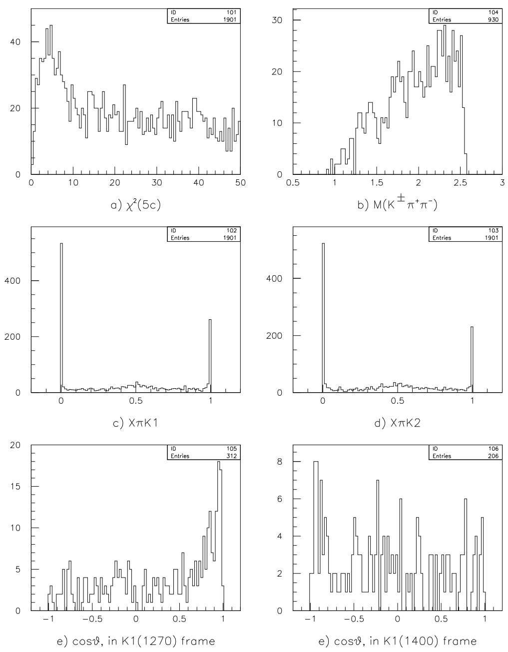

Figure 15: Distributions of precut values of the variables used for the $J/\psi \to K^+K^-\pi^+\pi^-$ selection.

6.2 $J/\psi \to K^+K^-\pi^+\pi^-$ invariant mass distributions

Figure 16a shows a scatterplot of $\pi^+\pi^-$ (vertical) $K^\pm\pi^+\pi^-$ (horizontal) masses for the selected events (two entries per event). Figure 16b shows the $\pi^+\pi^-$ mass distribution. There is some sign of a $\rho(770)$ in the $\pi^+\pi^-$ mass histogram, but not much evident clustering of events in the scatterplot. Figure 16c shows the $K^\pm\rho^0$ mass plot, where the ρ^0 is taken to be $\pi^+\pi^-$ pairs within ± 0.150 GeV of the nominal ρ mass. The $K_1(1270)$ signal, if any, is immersed in a heavy backround. (The $J/\psi \to K^\pm\rho^0$ distribution of Fig. 16c should be compared with the $\psi' \to K^\pm\rho^0$ distribution of Fig. 3c.) The peak near $M \simeq 1.4$ GeV could be due to the $K_1(1400)$. Even though this resonance decays primarily to $K^*\pi$, the $\pi^+\pi^-$ final state frequently has an invariant mass that lies within the ρ cut.

Figure 16d shows a scatterplot of $K^\pm\pi^\mp$ (vertical) vs $K^\pm\pi^+\pi^-$ (horizontal) masses for the selected events (four entries/event). There are two entries per event. Figure 16e shows the $K^\pm\pi^\mp$ mass distribution (two entries/event). Here the $K^*(890)$ is evident both as a horizontal band in the scatterplot and a peak in the $K\pi$ mass histogram. Figure 16f shows the $K^{*0}\pi^\pm$ mass distribution, where the K^* is taken to be $K^\pm\pi^\mp$ pairs within ± 0.050 GeV of the nominal K^{*0} mass. There is clear peaking of events near 1.4 GeV, indicating the presence of the $K_1(1400)$. (The $J/\psi \to K^{*0}\pi^\pm$ distribution of Fig. 16f should be compared with the corresponding distribution for ψ' decays shown in of Fig. 3f.)

7 $J/\psi \to K_1^+K^-$ acceptance

The acceptance and the efficiency for the analysis cuts are evaluated by means of a sample of simulated Monte Carlo events. We generated $10,000$ $\psi' \to \pi^+\pi^- J/\psi; J/\psi \to K_1^+(1270)K^-$ with subsequent $K_1^+(1270) \to K^+\rho^0; \rho^0 \to \pi^+\pi^-$ decays with flat angular distributions, and 10,000 with $K_1^+(1270) \to K^*\pi; K^{*0} \to K^+\pi^-$. We generated 100,000 $\psi' \to \pi^+\pi^- J/\psi; J/\psi \to K_1^+(1400)K^-$ with subsequent $K_1^+(1400) \to K^{*0}\pi \to K^+\pi^+\pi^-$ decays, and 50,000 $\psi' \to \pi^+\pi^- J/\psi; J/\psi \to K_1^+(1400)K^-$ with $K_1^+(1400) \to K^+\rho^0 \to K^+\pi^+\pi^-$ decays, also with flat angular distributions. The generated events were passed through a Monte Carlo simulation of the BES detector that generates simulated detector responses. The simulated data are analyzed by the same programs that are used for the data.

The $K\rho$ mass distribution for the events in the first sample that survive all the cuts

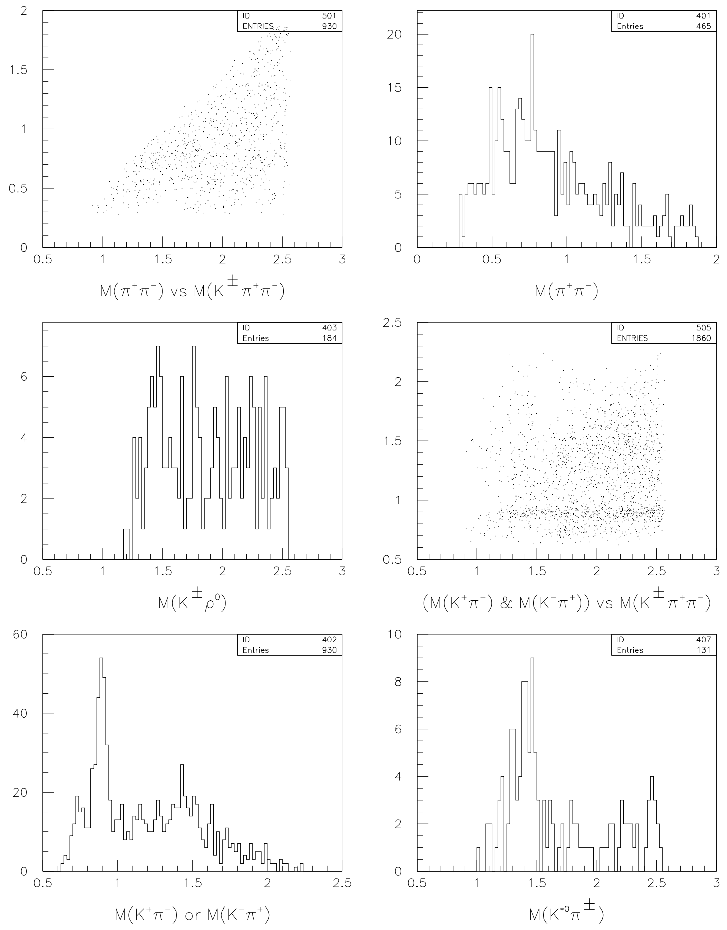

Figure 16: **a)** a) A scatterplot of $\pi^+\pi^-$ (vertical) vs $K^\pm\pi^+\pi^-$ (horizontal) masses for selected events. The **b)** $\pi^+\pi^-$ and **c)** K_ρ mass distributions. **d)** A scatterplot of $K^\pm\pi^\mp$ (vertical) vs $K^\pm\pi^+\pi^-$ (horizontal) masses for selected events. The **e)** $K\pi$ and **f)** $K^*\pi$ mass distributions.

is fit to the same $f_{K\rho}$ function, yielding an acceptance for this mode of $\eta_{K\rho}^{K_1(1270)\to K\rho} = 0.030 \pm 0.002$ (see Fig. 17). $K_1(1270)$ can also decay to $K^*\pi$, and the $K\rho$ and $K^*\pi$ cuts are not mutually exclusive. Therefore some of the $K_1(1270)$ in the $K\rho$ distribution, is due to the $K^*\pi$. The efficiency of this contribution is $\eta_{K^*\pi/K\rho}^{K_1(1270)\to K^*\pi} = 0.012 \pm 0.001$ (see Fig. 18).

The $K^*\pi$ mass distribution from the $K_1(1400)$ sample are fit to an s-wave Breit Wigner function. The acceptance is $\eta_{K^*\pi}^{K_1(1400)\to K^*\pi} = 0.029 \pm 0.000$ (see Fig. 19). We also measured $\eta_{K\rho/K^*\pi}^{K_1(1400)\to K\rho} = 0.007 \pm 0.001$.

To recapitulate:

$\eta_{K\rho}^{K_1(1270)\to K\rho} = 0.030 \pm 0.002$ (10,000 events)

$\eta_{K^*\pi/K\rho}^{K_1(1270)\to K^*\pi} = 0.012 \pm 0.001$ (10,000 events)

$\eta_{K^*\pi}^{K_1(1400)\to K^*\pi} = 0.029 \pm 0.000$ (100,000 events)

$\eta_{K\rho/K^*\pi}^{K_1(1400)\to K\rho} = 0.007 \pm 0.001$ (50,000 events)

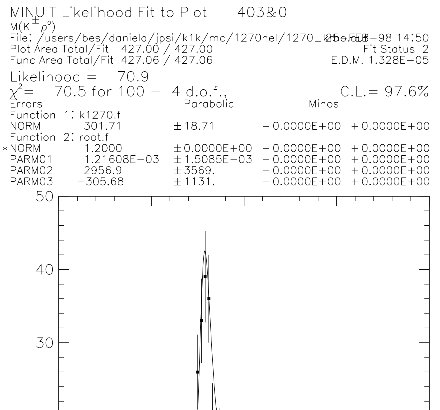

Figure 17: MC: $J/\psi \to K_1(1270)K, K_1(1270) \to K\rho^0$. Fit to the $K^+\rho^0$ mass distribution. (10,000 events)

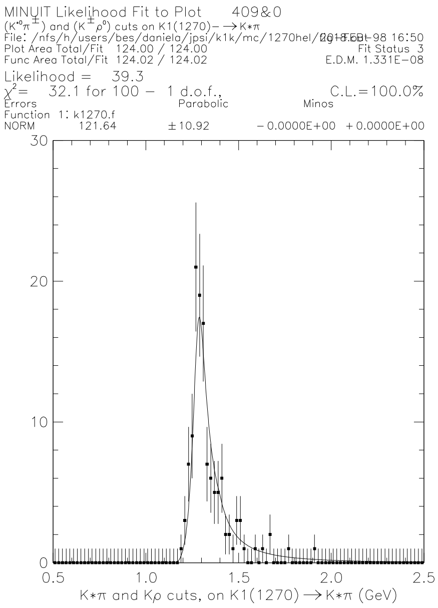

Figure 18: MC: $J/\psi \to K_1(1270)K, K_1(1270) \to K^*\pi$. Fit to the $K\rho^0$ mass distribution. (10,000 events)

8 $J/\psi \to K_1(1270)K$

8.1 Fit to the $K_1(1270) \to K\rho$ mass distribution.

We determine the number of $K_1(1270)$ events by fitting the $K\rho$ mass spectrum of Fig. 16c. There is scarce evidence for a $K_1(1270)$ in the heavy background.
Given that $K_1(1400) \to K^*\pi$ has a high branching fraction $(94 \pm 6)\%$, and $K_1(1400) \to K\rho$ has a very small branching fraction $(3 \pm 3)\%$, we infere that the slight $K_1(1400)$ in the $K\rho$ distribution, is due to a $K_1(1400) \to K^*\pi$, whose events are included in the $K\rho$ cuts.
To determine the shape of the $K_1(1400)$, we apply a $K\rho$ cut to the simulated $K_1(1400) \to K^*\pi$, which passed the $K^*\pi$ cut. (See Fig. 21). The Breit Wigner fit, yields a value of approximately 1.41 GeV for the mass, and of 0.13 GeV for the width.
Then we fit the data, using a $f_{k\rho}$, fixed at the PDG values for the $K_1(1270)$, and an s-wave Breit Wigner function fixed at the values determined from the Monte Carlo. We add the same background function we used for the $\psi' \to K_1(1270)K$, and we find $N_{evts}(1270) = 7.8 \pm 5.9$ (See Fig. 22). These events correspond to a limit of $N_{evts}^{(1270)} < 15.3$, at the 90% CL.

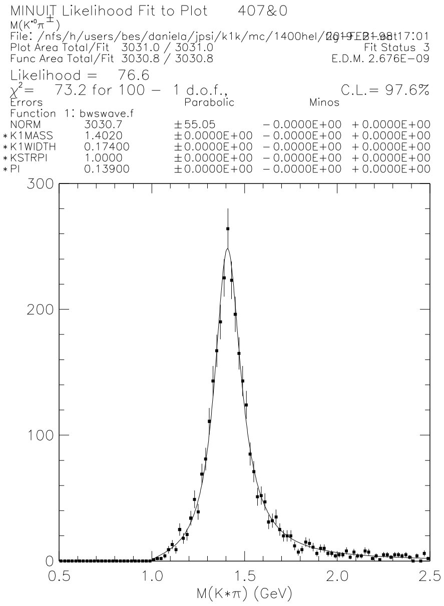

Figure 19: MC: $J/\psi \to K_1(1400)K, K_1(1400) \to K^*\pi$. Fit to the $K^*\pi$ mass distribution, 100,000 evts

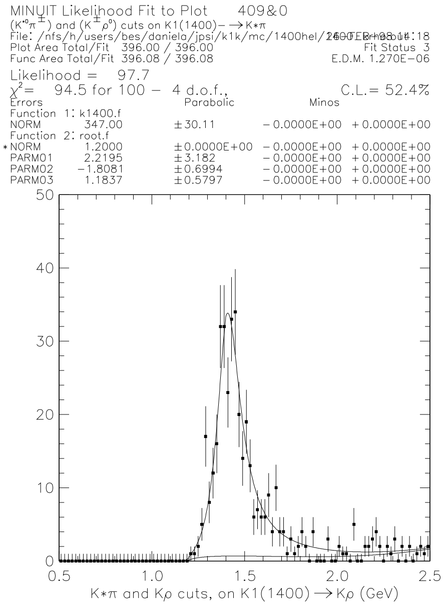

Figure 20: MC: $J/\psi \to K_1(1400)K, K_1(1400) \to K\rho$. Fit to the events with mass distribution included both within the $K\rho$ and the $K^*\pi$ cuts. (50,000 events)

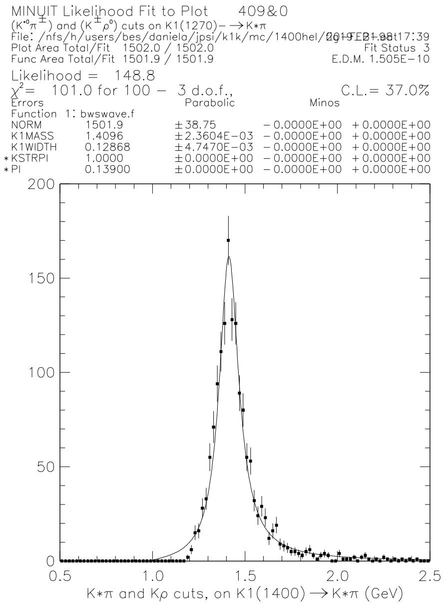

Figure 21: MC: $J/\psi \to K_1(1400)K, K_1(1400) \to K^*\pi$. Fit to the events with mass distribution included both within the $K\rho$ and the $K^*\pi$ cuts. (100,000 events)

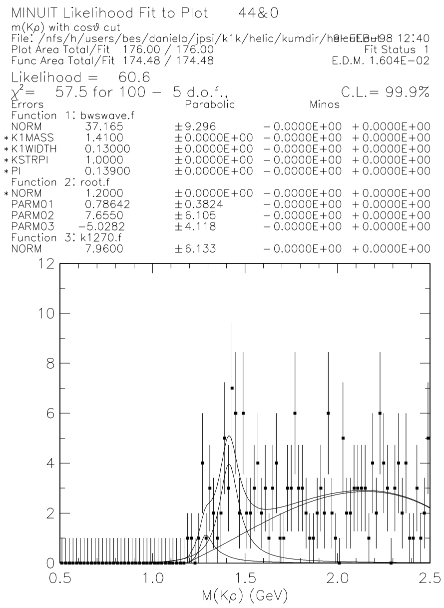

Figure 22: J/ψ Data: Fit to the $K\rho$ mass distribution, using a $f_{k\rho}$ fixed at the PDG values for the $K_1(1270)$, an s-wave Breit Wigner with mass and width determined by the MC, and a smooth background function at higher masses.

8.1.1 $J/\psi \to K_1(1270)^+K^-$ branching ratio

Using the relation

$$Br(J/\psi \;\; \to \;\; K_1^+(1270)K^- \; + \; cc); \qquad via \;\; (K_1(1270) \to K\rho) \tag{19}$$

$$= \frac{N_{evts}^{(1270)}}{\alpha[\eta_{K\rho}^{(K_1(1270)\to K\rho)} Br_{K_1(1270)\to K\rho\to K^+\pi^+\pi^-} + \eta_{K^*\pi/K\rho}^{(K_1(1270)\to K^*\pi)} Br_{K_1(1270)\to K^*\pi\to K^+\pi^+\pi^-}]} \tag{20}$$

where $\alpha = N_{\psi'}Br(\psi' \to \pi^+\pi^-J/\psi) = (1.1 \pm 0.1)10^6$ and $Br(\psi' \to \pi^+\pi^-J/\psi) = 0.324 \pm 0.026$ [5], we determine the branching ratio limit result

$$Br(J/\psi \to K_1^+(1270)K^- \; + \; cc) < 2.7 \times 10^{-3} \;\; 90\% \; CL \tag{21}$$

9 $J/\psi \to K_1(1400)K$

9.1 Fit to the $K_1(1400) \to K^*\pi$ mass distribution.

We fit the region $K^{*0}\pi^{\pm}$ mass distribution of Fig. 16 f, to an s-wave Breit Wigner with mass and width fixed at the PDG values for the K_1 (1400) ($m_{K1} = 1.402$ GeV and $\Gamma_{K1} = 0.174$ GeV), plus the usual background function.

The resulting fit, shown in Fig. 23, gives 58.6 ± 13.2 $K_1(1400)$ events.

9.2 $J/\psi \to K_1(1400)^+K^-$ branching ratio

Using the relation

$$Br(J/\psi \;\; \to \;\; K_1^+(1400)K^- \; + \; cc); \qquad via \;\; (K_1(1400) \to K^*\pi) \tag{22}$$

$$= \frac{N_{evts}^{(1400)}}{\alpha[\eta_{K^*\pi}^{(K_1(1400)\to K^*\pi)} Br_{K_1(1400)\to K^*\pi\to K^+\pi^+\pi^-} + \eta_{K\rho/K^*\pi}^{(K_1(1400)\to K\rho)} Br_{K_1(1400)\to K\rho\to K^+\pi^+\pi^-}]} \tag{23}$$

we derive

$$Br(J/\psi \to K_1^+(1400)K^- \; + \; cc) = (4.3 \pm 1.0 \pm 2.0) \times 10^{-3}, \tag{24}$$

The statistical error is based on the error on $N_{evts}^{(1400)}$, as obtained from the fit.

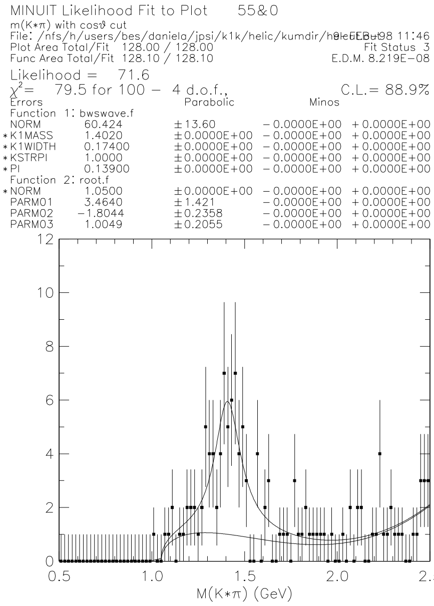

Figure 23: J/ψ Data: Fit to the $K^{*}\pi$ mass distribution using an s-wave Breit Wigner with mass and width fixed at the PDG values for the $K_1(1400)$ and a smooth background function

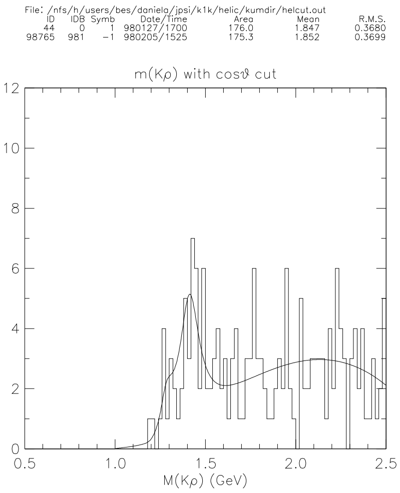

Figure 24: Contour shape of the plot shown in Fig. 22

.

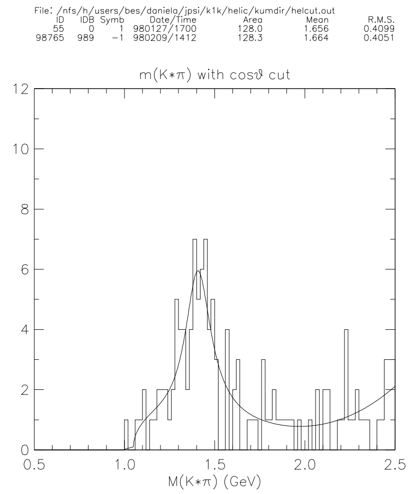

Figure 25: Contour shape of the plot shown in Fig. 23

.

10 Summary

We have measured the $\psi' \to AP$ decay branching ratios

- $Br(\psi' \to K_1^+(1270)K^- \ + \ cc) = (8.4 \pm 1.9 \pm 1.7) \times 10^{-4}$; and
- $Br(\psi' \to K_1^+(1400)K^- \ + \ cc) < 2.7 \times 10^{-4}$ 90% CL.

We find that AP decays are dominant exclusive hadron channels for the ψ'. The discrepancy between the $K_1(1270)$ and $K_1(1400)$ rates is contrary to expectations based on flavor-SU(3).

We have made a first measurement of J/ψ decays to strange AP final states:

- $Br(J/\psi \to K_1^+(1270)K^- \ + \ cc) < 2.7 \times 10^{-3}$ 90% CL and
- $Br(J/\psi \to K_1^+(1400)K^- \ + \ cc) = (4.3 \pm 1.0 \pm 2.0) \times 10^{-3}$.

Together with the $b_1\pi$, the $K_1(1270)\overline{K}$ channel is another observation of an exclusive ψ' hadronic decay channel that is enhanced relative to the J/ψ in the context of the 14% rule. In addition, the flavor-SU(3)-violating $K_1(1270)$-$K_1(1400)$ asymmetry has an opposite character for the ψ' and J/ψ. This can not be accommodated by adjustments of the singlet-triplet mixing angle.

11 Acknowledgements

We acknowledge the patient help and assistance of the members of the BES ψ' analysis groups at IHEP and at the University of Hawaii. This research is supported by the U.S. Department of Energy research grant number DE-FG03-94ER40833.

References

[1] M.E.B. Franklin *et al.* (Mark II Collaboration), Phys. Rev. Lett. **51**, 963 (1983).

[2] J.Z. Bai *et al.* (BES Collaboration), *Search for $\psi' \rightarrow$ Vector + Pseudoscalar Decays*, paper submitted to the 1995 International Symposium on Lepton and Photon Interactions at High Energies, Beijing, China.

[3] J.Z. Bai *et al.* (BES Collaboration), *Observation of New Anomalous Charmonium Decays*, paper submitted to the 1995 International Symposium on Lepton and Photon Interactions at High Energies, Beijing, China.

[4] See, for example, H.G. Blundell, S. Godfrey, and B. Phelps, Phys. Rev. **53**, 3712 (1996), M. Suzuki, Phys. Rev. **D47**, 1252 (1993), and references cited therein.

[5] L. Montanet *et al.* (Particle Data Group), Phys. Rev. **D50**, 1173 (1994).

[6] J.Z. Bai *et al.* (BES Collaboration), Nucl. Instr. and Meth. **A344**, 319 (1994) and Phys. Rev. Lett. **69**, 3021 1992.

[7] J.E. Augustin *et al.* (DM2 Collaboration), Nucl. Phys. **B320**, 1 (1989).

[8] J.Z. Bai *et al.* (BES Collaboration), *Branching Fractions for ψ' Decays to Octet-Baryon Pairs*, paper submitted to the 1995 International Symposium on Lepton and Photon Interactions at High Energies, Beijing, China.

[9] W.M. Dunwoodie, private communication.